

# Sparsity-based single-shot subwavelength coherent diffractive imaging

A. Szameit<sup>1,2†</sup>, Y. Shechtman<sup>1†</sup>, E. Osherovich<sup>3†</sup>, E. Bullkich<sup>1</sup>, P. Sidorenko<sup>1</sup>, H. Dana<sup>4</sup>, S. Steiner<sup>2</sup>, E. B. Kley<sup>2</sup>, S. Gazit<sup>1</sup>, T. Cohen-Hyams<sup>5</sup>, S. Shoham<sup>4</sup>, M. Zibulevsky<sup>3</sup>, I. Yavneh<sup>3</sup>, Y. C. Eldar<sup>6</sup>, O. Cohen<sup>1</sup> and M. Segev<sup>1\*</sup>

**Coherent Diffractive Imaging (CDI) is an algorithmic imaging technique where intricate features are reconstructed from measurements of the freely diffracting intensity pattern. An important goal of such lensless imaging methods is to study the structure of molecules that cannot be crystallized. Ideally, one would want to perform CDI at the highest achievable spatial resolution and in a single-shot measurement such that it could be applied to imaging of ultrafast events. However, the resolution of current CDI techniques is limited by the diffraction limit, hence they cannot resolve features smaller than one half the wavelength of the illuminating light. Here, we present sparsity-based single-shot subwavelength resolution CDI: algorithmic reconstruction of subwavelength features from far-field intensity patterns, at a resolution several times better than the diffraction limit. This work paves the way for subwavelength CDI at ultrafast rates, and it can considerably improve the CDI resolution with X-ray free-electron lasers and high harmonics.**

Improving the resolution in imaging and microscopy has been a driving force in the natural sciences for centuries. Fundamentally, the propagation of an electromagnetic field in a linear medium can be fully described through the propagation of its eigenmodes (a complete and orthogonal set of functions that do not exchange power during propagation). In homogeneous, linear and isotropic media, the most convenient set of eigenmodes are simply plane waves, each characterized by its spatial frequency and associated propagation constant. However, when light of wavelength  $\lambda$  propagates in media with refractive index  $n$ , only spatial frequencies below  $n/\lambda$  can propagate, whereas all frequencies above  $n/\lambda$  are rendered evanescent and decay exponentially with propagation distance. Hence, for propagation distances larger than  $\lambda$ , diffraction in a homogeneous medium acts as a low-pass filter. Consequently, optical features of subwavelength resolution are highly blurred in a microscope, owing to the loss of information carried by their higher spatial frequencies<sup>1,2</sup>. Over the years, numerous ‘hardware’ methods for subwavelength imaging have been demonstrated<sup>3–10</sup>; however, all of them rely on multiple exposures, either through mechanical scanning (for example, scanning near-field microscope<sup>3,4</sup>, scanning a subwavelength ‘hot spot’<sup>5–7</sup>), or by using scanning or ensemble-averaging over multiple experiments with fluorescent particles<sup>8–10</sup>. Apart from hardware solutions, several algorithmic approaches for subwavelength imaging have been suggested (see, for example refs 11–13). Basically, algorithmic subwavelength imaging aims to reconstruct the extended spatial frequency range (amplitudes and phases) of the information (‘signal’) from measurements which are fundamentally limited to the range  $[-n/\lambda, n/\lambda]$  in the plane-wave spectrum. However, as summarized in Goodman’s 2005 book<sup>14</sup>, “all methods for extrapolating bandwidth beyond the diffraction limit are known to be extremely sensitive to both noise in the

measured data and the accuracy of the assumed a priori knowledge” such that “it is generally agreed that the Rayleigh diffraction limit represents a practical frontier that cannot be overcome with a conventional imaging system”.

Despite this commonly held opinion that algorithmic methods for subwavelength imaging are impractical<sup>14</sup>, we have recently proposed a method for reconstructing subwavelength features from the far-field (and/or blurred images) of sparse optical information<sup>15</sup>. The concept of sparsity-based subwavelength imaging is related to compressed sensing (CS), which is a relatively new area in information processing<sup>16–20</sup>. We have shown that our sparsity-based method works for both coherent<sup>15,21</sup> and incoherent<sup>22,23</sup> light, and presented an experimental proof of concept<sup>15,22</sup>: the recovery of fine features that were cut off by a spatial low-pass filter. Subsequently, we took these concepts into the true subwavelength domain and experimentally demonstrated resolutions several times better than the diffraction limit: the recovery of 100 nm features illuminated by 532 nm wavelength light<sup>21</sup>. These ideas were followed by several groups, most notably the recent demonstration of sparsity-based super-resolution of biological specimens<sup>24</sup>.

Here, we take the sparsity-based concepts into a new domain, and present the first experimental demonstration of subwavelength CDI: single-shot recovery of subwavelength images from far-field intensity measurements. Recalling that CDI is an algorithmic imaging technique to reconstruct features from measurements of the freely diffracting intensity pattern<sup>25–32</sup>, what we demonstrate here is sparsity-based subwavelength imaging combined with phase retrieval at the subwavelength level. We recover the subwavelength features without measuring (or assuming) any phase information whatsoever; the only measured data at our disposal is the intensity of the diffraction pattern (Fourier power spectrum) and the support structure of the blurred image. Our processing

<sup>1</sup>Physics Department and Solid State Institute, Technion, Haifa 32000, Israel, <sup>2</sup>Institute of Applied Physics, Friedrich-Schiller-Universität Jena, Max-Wien-Platz 1, 07743 Jena, Germany, <sup>3</sup>Computer Science Department, Technion, 32000 Haifa, Israel, <sup>4</sup>Department of Biomedical Engineering, Technion, Haifa 32000, Israel, <sup>5</sup>Microelectronics Research Center, Department of Electrical Engineering, Technion, Haifa 32000, Israel, <sup>6</sup>Department of Electrical Engineering, Technion, Haifa 32000, Israel. †These authors contributed equally to this work. \*e-mail: msegev@technion.ac.il

scheme combines bandwidth extrapolation and phase retrieval, considerably departing from classical CS. We therefore devise a new sparsity-based algorithmic technique that facilitates robust subwavelength CDI under typical experimental conditions.

### Sparsity-based super-resolution

In mathematical terms, the bandwidth extrapolation problem underlying subwavelength imaging corresponds to a non-invertible system of equations which has an infinite number of solutions, all producing the same (blurred) image carried by the propagating spatial frequencies. That is, after measuring the far-field, one can add any information in the evanescent part of the spectrum while still being consistent with the measured image. Of course, only one choice corresponds to the correct subwavelength information that was cut off by the diffraction limit. The crucial task is therefore to extract the one correct solution out of the infinite number of possibilities for bandwidth extension. This is where sparsity comes into play. Sparsity presents us with prior information that can be exploited to resolve the ambiguity resulting from partial measurements and identify the correct bandwidth extrapolation that will yield the correct recovery of the subwavelength image.

Information is said to be sparse when most of its projections onto a complete set of base functions are zero (or negligibly small). For example, an optical image is sparse in the near-field when the number of non-zero pixels is small compared with the entire field of view. However, sparsity need not necessarily be in a near-field basis; rather, it can be in any mathematical basis. Many images are indeed sparse in an appropriate basis. In fact, this is the logic behind many popular image compression techniques, such as JPEG. In the fields of signal processing and coding theory, it has been known for some time that a sparse signal can be precisely reconstructed from a subset of measurements in the Fourier domain, even if the sampling is carried out entirely in the low-frequency range<sup>33</sup>. This basic result was extended<sup>16</sup> to the case of random sampling in the Fourier plane and initiated the area of CS. An essential result of CS is that, in the absence of noise, if the 'signal' (information to be recovered) is sparse in a basis that is sufficiently uncorrelated with the measurement basis, then searching for the sparsest solution (that conforms to the measurements) yields the correct solution. In the presence of noise (that is not too severe), the error is bounded, and many existing CS algorithms can recover the signal in a robust fashion under the same assumptions.

The concept underlying sparsity-based super-resolution imaging<sup>15,21–23</sup> and sparsity-based CDI relies on the advance knowledge that the optical object is sparse in a known basis. The concept yields a method for bandwidth extrapolation. Namely, sparsity makes it possible to identify the continuation of the truncated spatial spectrum that yields the correct image. As we have shown in ref. 15, sparsity-based super-resolution imaging departs from standard CS, because the measurements are forced to be strictly in the low-pass regime, and therefore cannot be taken in a more stable fashion, as generally required by CS. Therefore, we developed a specialized algorithm, non-local hard thresholding (NLHT), to reconstruct both amplitude and phase from low-frequency measurements<sup>15</sup>. However, NLHT, as well as other CS techniques necessitate the measurement of the phase in the spectral domain. In contrast, the current problem of subwavelength CDI combines phase retrieval with subwavelength imaging, where we aim to extrapolate the bandwidth from amplitude measurements alone. Mathematically, this problem can be viewed in principle as a special case of quadratic CS, introduced in ref. 23. However, the algorithm suggested in ref. 23 is designed for a more general problem, resulting in high computational complexity. Here we devise a specific algorithm that directly treats the problem at hand.

### Sparsity-based subwavelength CDI

For the current case of subwavelength CDI, the phase information in the spectral domain is not available. Hence, fundamentally, subwavelength CDI involves both bandwidth extrapolation and phase retrieval. However, despite the missing phase, which carries extremely important information, we show that sparsity-based ideas can still make it possible to identify the correct extrapolation. Namely, if we know that our signal is sufficiently sparse in an appropriate basis, then—from all the possible solutions which could create the truncated spectrum—the correct extrapolation is often the one yielding the maximally sparse signal. Moreover, even under real experimental conditions, that is, in the presence of noise, searching for the sparsest solution that is consistent with the measured data often yields a reconstruction that is very close to the ideal one.

Our algorithm iteratively reveals the support of the sought image by sequentially rejecting less likely areas (circles, in the experiments shown below). Thus, the sparsity of the reconstructed image increases with each iteration loop. This process continues as long as the reconstructed image yields a power spectrum that remains in good agreement with the measurements. The process stops when the reconstructed power spectrum deviates from the measurements by some threshold value. However, it is important to emphasize that the exact threshold value and the degree of sparseness of the sought image need not be known a priori, as our method provides a natural termination criterion. Namely, the correct reconstruction is identified automatically. The algorithms work rather fast: our straightforward implementation in MATLAB requires 25–60 s (depending on the image) on an Intel i7-2600 CPU. These times can be reduced to sub-seconds with some effort put into software optimization.

A detailed description of the reconstruction method, as well as a comparison with other methods (that do not exploit sparsity), are provided in the Supplementary Information.

### Finding a suitable basis

As explained above, sparsity-based CDI relies on the advance knowledge that the object is sparse in a known basis. In some cases, the 'optimal' basis—the basis in which the object is represented both well and sparsely—is known from physical arguments. For example, the features in very large scale integration (VLSI) chips are best described by pixels on a grid, because they obey certain design rules. In this case a suitable basis would be comprised of rectangular segments typical of VLSI chips. In some cases, however, the prior knowledge about the optimal basis is more loose; namely, it may be known that the object is well and sparsely described in a basis that belongs to a certain family of bases. For example, one may know in advance that the object is sparse in the near-field using a rectangular grid, yet the optimal grid spacing is not known a priori. We address this issue in Supplementary Section S4, where we describe a sparsity-based method that uses the experimental data to algorithmically find the optimal grid size (optimal basis) for our subwavelength CDI technique. That section also shows that the choice of basis functions is not particularly significant in our procedure: we obtain very reasonable reconstruction with almost any choice of basis functions, as long as they conform to the optimal grid. Finally, we note that recent work has shown that it is often possible to find the basis from a set of low-resolution images, using 'blind CS'<sup>34</sup>. Likewise, in situations where a sufficient number of images of a similar type are available at high resolution, one can construct a near-optimal basis through dictionary learning algorithms<sup>35</sup>.

### Experiments

We demonstrate the subwavelength CDI technique experimentally on two-dimensional (2D) structures. The optical information is generated in our optical microscope, where a laser beam at  $\lambda = 532$  nm illuminates our subwavelength sample, using a NA = 0.8

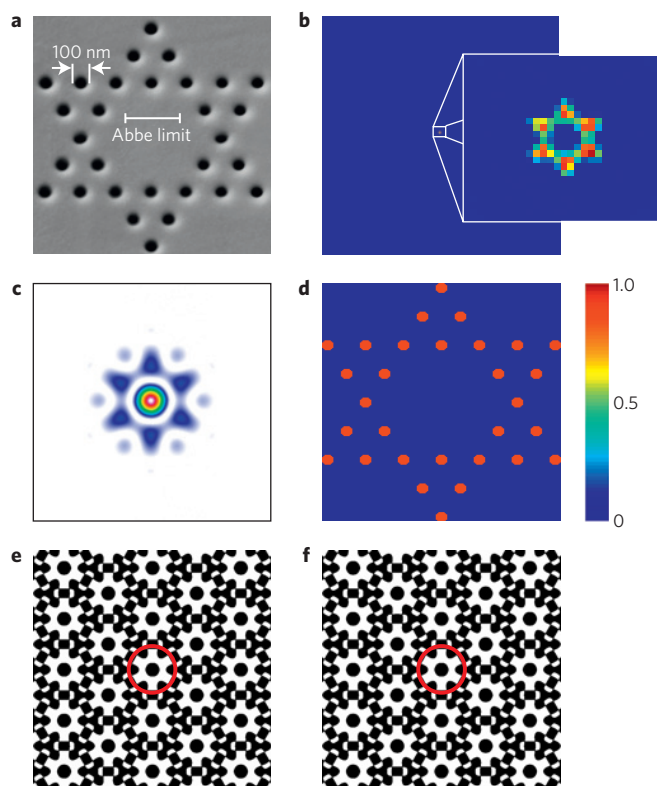


**Figure 1 | Reconstruction of two-dimensional subwavelength information.**

**a**, SEM image of the sample. **b**, The blurred image, as seen in the microscope. The individual holes cannot be resolved. **c**, The measured spatial power spectrum of the field. The colour map is identical to that in the other panels: only the background has been removed for clarity. **d**, The reconstructed 2D information, algorithmically recovered from the measured power spectrum (**c**) and the blurred image (**b**). **e**, The algorithmically recovered phase in the spatial spectrum domain. White represents zero-phase, whereas black denotes  $\pi$ -phase. **f**, The phase in the spectral domain calculated from the Fourier transform of **a**. The red circle in **e**, and **f** marks the cut-off frequency imposed by the diffraction limit. The phase structure recovered algorithmically by sparsity-based CDI reconstruction, shown in **e**, coincides with the phase structure shown in **f**, which was calculated from the SEM image of **a**, both within the red circle (where the power spectrum is measured) and outside it (where it corresponds to evanescent waves, which are lost owing to the diffraction limit, never reaching the camera). Clearly, our sparsity-based CDI technique correctly recovers both the evanescent waves (amplitude and phase) and the phase of the propagating waves.

( $\times 40$ ) water immersion microscope objective. The transmitted light is collected using a NA = 1.0 ( $\times 60$ ) water immersion microscope objective, and projected on a camera using a single optical lens. The blurred image and the truncated spatial power spectrum (absolute value squared of the Fourier transform) are measured by positioning the camera in the image plane and the Fourier plane of the imaging system, respectively. The experimental set-up is sketched in the Supplementary Information, along with a detailed description of the apparatus.

The samples, which consist of arrangements of nano-holes of diameter 100 nm each, is made of a 100-nm-thick layer of chromium on glass; this thickness is larger than the skin depth at optical frequencies, such that the samples are opaque except for the holes.

We begin with an ordered structure: a Star of David, consisting of 30 nano-holes. Figure 1a shows a scanning electron microscope (SEM) image of this sample. Figure 1b shows the image seen

in the microscope. As expected, the image is small and severely blurred. The measured truncated spatial power spectrum, as shown in Fig. 1c, covers a large area on the camera detector, therefore facilitating a much higher number of meaningful measurements (each pixel corresponds to one measurement). We emphasize that only intensity measurements are used, in both the (blurred) image plane and in the (truncated) Fourier plane (Fig. 1b,c, respectively), without measuring (or assuming) the phase anywhere. The recovered image, using our sparsity-based algorithm, is shown in Fig. 1d. Clearly, we recover the correct number of circles, their positions, their amplitudes, and the entire spectrum (amplitude and phase), including the large evanescent part of the spectrum. This demonstrates subwavelength CDI: image reconstruction combined with phase retrieval at the subwavelength scale. Moreover, as explained in the Supplementary Information, the intensity of the blurred image (Fig. 1b) is used only for rough estimation of the image support. Our reconstruction method yields better results than other phase-retrieval algorithms (see comparisons in the Supplementary Information), because it exploits the sparsity of the signal (the image to be recovered) as prior information. As mentioned earlier, the underlying logic is to minimize the number of degrees of freedom, while always conforming to the measured data, which in this case is the truncated power spectrum (intensity in Fourier space). In the example presented in Fig. 1, we take the data from Fig. 1b,c, search for the sparsest solution in the basis of circles of 100 nm diameter on a grid, and reconstruct a perfect Star of David, as shown in Fig. 1d. The grid is rectangular with 100 nm spacing (Supplementary Section S4 describes how this parameter is found automatically), where the exact position of the grid with respect to the reconstructed information is unimportant (see Supplementary Information).

We emphasize that our reconstruction algorithm is able to reconstruct the phase in the spatial spectrum domain (the Fourier transform) from the intensity measurement in Fourier space and some rough estimation of the image support. In addition, we use the knowledge that the holes are illuminated by a plane wave, implying that the image is real and non-negative in real space. However, we do not use any prior knowledge about the relative amplitudes of the light passing the holes. In this Star of David example, our algorithm reconstructs the phase in the spectral plane, as presented in Fig. 1e. For comparison, Fig. 1f shows the phase distribution in Fourier space, as obtained numerically from the ideal model of the subwavelength optical information (calculated from the SEM image of Fig. 1a). The red circle in Fig. 1e,f marks the cut-off frequency imposed by the diffraction limit. The phase structure recovered by our sparsity-based CDI algorithm, shown in Fig. 1e, coincides with the phase structure shown in Fig. 1f, both within the red circle (where the power spectrum is measured) and outside it (where it corresponds to the evanescent waves, which never reach the camera). Clearly, our sparsity-based CDI technique recovers correctly both the evanescent waves (amplitude and phase) and the phase of the propagating waves. The reconstruction in Fig. 1 therefore constitutes the first demonstration of subwavelength CDI.

Interestingly, when comparing the Fourier transform of the sample with the measured spatial power spectrum, one finds that more than 90% of the power spectrum is truncated by the diffraction limit, acting as a low-pass filter (Fig. 2). That is, we use the remaining 10% of the power spectrum and the blurred image to successfully reconstruct the subwavelength features with high accuracy. In other words, the prior knowledge of sparsity and the basis is overcoming the loss of information in 90% of the power spectrum. As demonstrated in the Supplementary Information, it is the sparsity prior that makes it happen: without assuming the sparsity prior the reconstruction suffers from large errors.

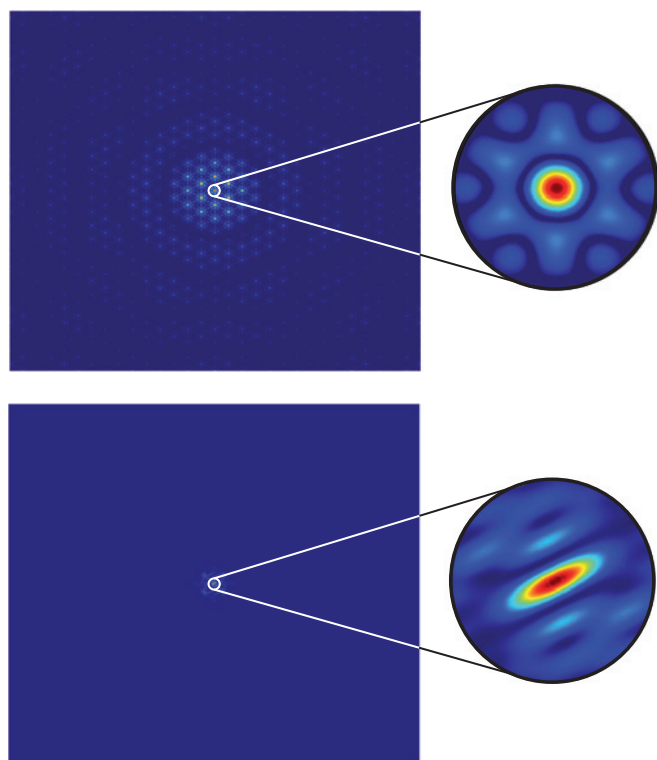


**Figure 2 | Truncation of the information by the transfer function.** Spatial power spectra of the fields forming the Star of David (upper row) and the irregular arrangement of holes (bottom row). The spectra are truncated by the diffraction limit (the white circle, corresponding to the zoom-in on the right), beyond which all spectral components are evanescent. The lost part contains about 92% of the total power in the case of the Star of David, and 74% in the case of the second (irregular) image.

The Star of David exhibits certain symmetries, which could in principle assist the phase retrieval had these symmetries been known. However, symmetry was not used for the reconstruction of the subwavelength features of Fig. 1. Nevertheless, it is illustrative to present another example with no spatial symmetry at all: an irregular arrangement of subwavelength holes on the assumed grid. Figure 3a shows the blurred image of an unknown number of subwavelength circles, distributed in a random manner. The respective Fourier power spectrum, as observed in the microscope, is shown in Fig. 3b. This sample is clearly not symmetric in real space, hence it does not exhibit a real Fourier transform. Still, we are able to reconstruct the subwavelength information, as shown in Fig. 3c, where all features of the original sample are retrieved, despite the inevitable noise in the experimental system. Figure 3d shows the SEM image of the sample, exhibiting the random arrangement of 100 nm holes. The electromagnetic field passing through these nano-holes has roughly the same amplitude for all the holes. The reconstructed amplitudes at the hole sites are represented by the colours in Fig. 3c, highlighting the fact that the reconstructed field has similar amplitude at all the holes. The reconstructed phase in the spectral plane is presented in Fig. 3e, where the white circle marks the cutoff imposed by the diffraction limit. As shown there, our algorithm recovers the phase throughout the entire Fourier plane, including the region of evanescent waves far away from the cutoff frequency. For comparison, Fig. 3f shows the phase distribution in Fourier space, as obtained numerically from the ideal model of the subwavelength optical information (calculated from the SEM image of Fig. 3d). Clearly, the correspondence between the original spectral phase and the reconstructed one is excellent, including in the deep evanescent regions. Interestingly, Fig. 3e also shows the

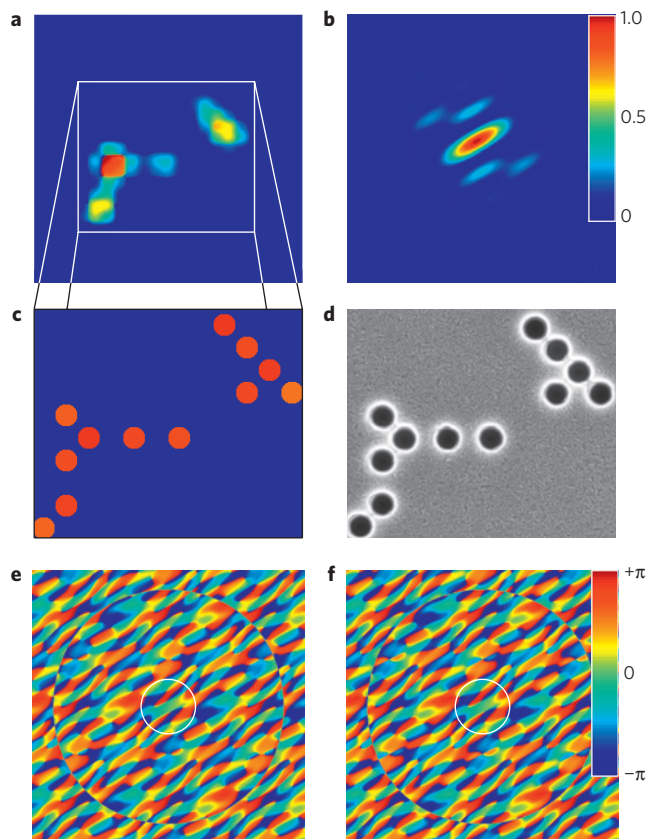


**Figure 3 | Reconstruction of an irregular arrangement of two-dimensional subwavelength holes.** **a**, The blurred image as seen in the microscope. **b**, The measured spatial power spectrum of the field. **c**, The algorithmically reconstructed 2D information, showing 12 holes in an irregular arrangement. **d**, SEM image of the sample depicting the irregular arrangement of nano-holes. **e**, The algorithmically recovered phase in the spatial spectrum domain. **f**, The phase in the spatial spectrum domain calculated from the Fourier transform of **d**.

correct reconstruction of the phase around the faint high-frequency circle (of radius  $\sim 4$  times the diffraction limit) where the phase jumps by  $\pi$ . Physically, this ‘phase-jump circle’ is located at the first zero of the Fourier transform of a circular aperture, which in Fourier space multiplies the phase distribution generated by the irregular positions of the holes. The excellent agreement between Fig. 3e and f highlights the strength of the sparsity-based algorithmic technique.

## Outlook

In this work, we presented a technique facilitating reconstruction of subwavelength features, along with phase retrieval at the subwavelength scale, at an unprecedented resolution for single-shot experiments. That is, we have taken coherent lensless imaging into the subwavelength scale, and demonstrated subwavelength CDI from intensity measurements alone. Because our method is based on single-shot experiments, it establishes the possibility of subwavelength CDI, and makes it suitable to work for ultrafast measurements, such as those carried out with X-ray free-electron lasers<sup>30,32</sup> and high-harmonic generation<sup>29</sup>.

Our method relies on prior knowledge—that the sample is sparse in a known basis (circles on a grid, in the examples in Figs 1–3). We emphasize that sparsity is what makes our phase retrieval work: the other assumptions used in the algorithm (non-negativity, bounded support and the known basis) alone are not sufficient. It is important to note that most natural and artificial objects are sparse, in some basis. The information does not necessarily have to

be sparse in real space: it can be sparse in any mathematical basis whose relation to the measurement basis is known, for example, the wavelet basis or the gradient of the field intensity, given that this basis is sufficiently uncorrelated with the measurements. In all these cases our technique can provide a major improvement by 'looking beyond the resolution limit' in a single-shot experiment. As our approach is purely algorithmic, it can be applied to every optical microscope and imaging system as a simple computerized image processing tool, with practically no extra hardware. The fact that our technique works in a single-shot holds the promise for ultrafast subwavelength imaging: one could capture a series of ultrafast blurred images, and then off-line processing will reveal their subwavelength features, which could vary from one frame to the next. Finally, we note that our technique is general, and can be extended also to other, non-optical, microscopes, such as atomic force microscopes, scanning tunnelling microscopes, magnetic microscopes, and other imaging systems. We believe that the microscopy technique presented here holds the promise to revolutionize the world of microscopy with just minor adjustments to current technology: sparse subwavelength images could be recovered by making efficient use of their available degrees of freedom. Last, but not least, we emphasize that our approach is more general than the particular subject of optical subwavelength imaging. It is in fact a universal scheme for recovering information beyond the cut-off of the response function of a general system, relying only on a priori knowledge that the information is sparse in a known basis. As an exciting example, we have recently investigated the ability to use this method for recovering the actual shape of very short optical pulses measured by a slow detector<sup>36</sup>. Our preliminary theoretical and experimental results indicate, unequivocally, that our method offers an improvement by orders of magnitude over the most sophisticated deconvolution methods. In a similar vein, we believe that our method can be applied for spectral analysis, offering a means to recover the fine details of atomic lines, as long as they are sparse (that is, do not form bands). In principle, the ideas described here can be generalized to any sensing/detection/data acquisition schemes, provided only that the information is sparse in a known basis, and that the measurements are taken in a basis sufficiently uncorrelated to it.

Received 30 November 2011; accepted 29 February 2012;  
published online 1 April 2012

## References

- Abbe, E. Beiträge zur Theorie des Mikroskops und der Mikroskopischen Wahrnehmung. *Arch. Mikrosk. Anatomie* **9**, 413–468 (1873).
- Lipson, S. G., Lipson, H. & Tannhauser, D. S. *Optical Physics* 3rd edn (Cambridge Univ. Press, 1995).
- Lewis, A., Isaacson, M., Haroutian, A. & Muray, A. Development of a 500-Å spatial-resolution light-microscope: I. Light is efficiently transmitted through  $\lambda/16$  diameter apertures. *Ultramicroscopy* **13**, 227–231 (1984).
- Betzig, E., Trautman, J. K., Harris, T. D., Weiner, J. S. & Kostelak, R. L. Breaking the diffraction barrier: Optical microscopy on a nanometric scale. *Science* **251**, 1468–1470 (1991).
- Di Francia, G. T. Super-gain antennas and optical resolving power. *Nuovo Cimento* **9**, 426–438 (1955).
- Lezec, H. J. *et al.* Beaming light from a subwavelength aperture. *Science* **297**, 820–823 (2002).
- Huang, F. M. & Zheludev, N. I. Super-resolution without evanescent waves. *Nano Lett.* **9**, 1249–1254 (2009).
- Hell, S. W. & Wichmann, J. Breaking the diffraction resolution limit by stimulated emission: Stimulated-emission-depletion microscopy. *Opt. Lett.* **19**, 780–783 (1994).
- Yildiz, A. *et al.* Myosin V walks hand-overhand: Single fluorophore imaging with 1.5 nm localization. *Science* **300**, 2061–2065 (2003).
- Hell, S. W., Schmidt, R. & Egner, A. Diffraction-unlimited three-dimensional optical nanoscopy with opposing lenses. *Nature Photon.* **3**, 381–387 (2009).

- Harris, J. L. Diffraction and resolving power. *J. Opt. Soc. Am.* **54**, 931–936 (1964).
- Papoulis, A. A new algorithm in spectral analysis and band-limited extrapolation. *IEEE Trans. Circuits Syst.* **22**, 735–742 (1975).
- Gerchberg, R. W. Super-resolution through error energy reduction. *J. Mod. Opt.* **21**, 709–720 (1974).
- Goodman, J. W. *Introduction to Fourier Optics* 3rd edn (Roberts, 2005).
- Gazit, S., Szameit, A., Eldar, Y. C. & Segev, M. Super-resolution and reconstruction of sparse subwavelength images. *Opt. Exp.* **17**, 23920–23946 (2009).
- Candes, E. J., Romberg, J. & Tao, T. Robust uncertainty principles: Exact signal reconstruction from highly incomplete frequency information. *IEEE Trans. Inf. Theory* **52**, 489–509 (2006).
- Donoho, D. L. Compressed sensing. *IEEE Trans. Inf. Theory* **52**, 1289–1306 (2006).
- Candes, E. J. & Tao, T. Near-optimal signal recovery from random projections: Universal encoding strategies? *IEEE Trans. Inf. Theory* **52**, 5406–5425 (2006).
- Candes, E. J. & Wakin, M. B. An introduction to compressive sampling. *IEEE Signal Process. Mag.* **25**, 21–30 (2008).
- Duarte, M. & Eldar, Y. C. Structured compressed sensing: From theory to applications. *Trans. Signal Process.* **59**, 4053–4085 (2011).
- Szameit, A. *et al.* Far-field microscopy of sparse subwavelength objects, Preprint at <http://arxiv.org/abs/1010.0631v1> (2010).
- Shechtman, Y., Gazit, S., Szameit, A., Eldar, Y. C. & Segev, M. Super-resolution and reconstruction of sparse images carried by incoherent light. *Opt. Lett.* **35**, 1148–1150 (2010).
- Shechtman, Y., Eldar, Y. C., Szameit, A. & Segev, M. Sparsity-based subwavelength imaging with partially spatially incoherent light via quadratic compressed sensing. *Opt. Exp.* **19**, 14807–14822 (2011).
- Derin, S. D., Wang, Z., Do, M. & Popescu, G. Cell imaging beyond the diffraction limit using sparse deconvolution spatial light interference microscopy. *Biomedical Opt. Exp.* **2**, 1815–1827 (2011).
- Sayre, D. Some implications of a theorem due to Shannon. *Acta Crystallogr.* **5**, 843 (1952).
- Miao, J., Charalambous, P., Kirz, J. & Sayre, D. Extending the methodology of X-ray crystallography to allow imaging of micrometer-sized non-crystalline specimens. *Nature* **400**, 342–344 (1999).
- Quiney, H. M. Coherent diffractive imaging using short wavelength light sources: A tutorial review. *J. Mod. Opt.* **57**, 1109–1149 (2010).
- Chapman, H. N. & Nugent, K. A. Coherent lensless X-ray imaging. *Nature Photon.* **4**, 833–839 (2010).
- Sandberg, R. L. *et al.* Lensless diffractive imaging using tabletop coherent high-harmonic soft-X-ray beams. *Phys. Rev. Lett.* **99**, 098103 (2007).
- Chapman, H. N. *et al.* Femtosecond time-delay X-ray holography. *Nature* **448**, 676–679 (2007).
- Neutze, R., Wouts, R., van der Spoel, D., Weckert, E. & Hajdu, J. Potential for biomolecular imaging with femtosecond X-ray pulses. *Nature* **406**, 752–757 (2000).
- Chapman, H. M. *et al.* Femtosecond X-ray protein nanocrystallography. *Nature* **470**, 73–77 (2011).
- Vetterli, M., Marziliano, P. & Blu, T. Sampling signals with finite rate of innovation. *IEEE Trans. Signal Process.* **50**, 1417–1428 (2002).
- Gleichman, S. & Eldar, Y. C. Blind compressed sensing. *IEEE Trans. Inform. Theory* **57**, 6958–6975 (2011).
- Aharon, M., Elad, M. & Bruckstein, A. K-SVD: An algorithm for designing overcomplete dictionaries for sparse representation. *IEEE Trans. Signal Process.* **54**, 4311–4322 (2006).
- Sidorenko, P. *et al.* *The 2010 Frontiers Optics Conference, OSA Technical Digest* (Optical Society of America, 2010), Paper FTuE2.

## Acknowledgements

This work was partially supported by an Advanced Grant from the European Research Council. A.S. thanks the Leopoldina—the German Academy of Natural Sciences for financial support (grant LPDS 2009-13). The research of O.C., E.B. and P.S. was supported by the Legacy Heritage Science Initiative Program ('MORASHA') of the Israel Science Foundation.

## Author contributions

All authors contributed significantly to the work presented in this paper.

## Additional information

The authors declare no competing financial interests. Supplementary information accompanies this paper on [www.nature.com/naturematerials](http://www.nature.com/naturematerials). Reprints and permissions information is available online at [www.nature.com/reprints](http://www.nature.com/reprints). Correspondence and requests for materials should be addressed to M.S.